Multiple pressure-induced transitions in HgCr2S4

Ilias Efthimiopoulos, Alexander Yaresko, Vladimir Tsurkan, Joachim Deisenhofer, Alois Loidl, Changyong Park, Yuejian Wang

Multiple pressure-induced transitions in HgCr$_2$S$_4$ ⊘

Ilias Efthimiopoulos; Alexander Yaresko; Vladimir Tsurkan; Joachim Deisenhofer; Alois Loidl; Changyong Park;
Yuejian Wang

Check for updates

View Online

Export Citation

Multiple pressure-induced transitions in HgCr$_2$S$_4$

Ilias Efthimiopoulos,[1,a)] Alexander Yaresko,[2] Vladimir Tsurkan,[3,4] Joachim Deisenhofer,[3] Alois Loidl,[3] Changyong Park,[5] and Yuejian Wang[1,b)]

[1]*Department of Physics, Oakland University, Rochester, Michigan 48309, USA*
[2]*Max Planck Institute for Solid State Research, D-70569 Stuttgart, Germany*
[3]*Experimental Physics 5, Center for Electronic Correlations and Magnetism, Institute of Physics,*
University of Augsburg, D-86159 Augsburg, Germany
[4]*Institute of Applied Physics, Academy of Sciences of Moldova, MD 2028 Chisinau, Republic of Moldova*
[5]*High Pressure Collaborative Access Team, Geophysical Laboratory, Carnegie Institution of Washington,*
Advanced Photon Source, Argonne National Laboratory, Argonne, Illinois 60439, USA

We have performed combined experimental and theoretical high-pressure investigations on magnetoelectric HgCr$_2$S$_4$ spinel. Overall, HgCr$_2$S$_4$ exhibits three reversible structural transitions under pressure: the starting Fd-$3m$ phase adopts a tetragonal $I4_1/amd$ structure at 20 GPa, an orthorhombic distortion occurs above 26 GPa, whereas a third structural transition takes place beyond 37 GPa. During the Fd-$3m$ to $I4_1/amd$ structural transition, HgCr$_2$S$_4$ experiences a volume change of 4% which is unexpected from space group symmetry considerations alone. Furthermore, the Fd-$3m$ to $I4_1/amd$ transformation appears to be concomitant with an insulator-to-metal transition whereas compression of HgCr$_2$S$_4$ leads to a gradual suppression of its ferromagnetism. © *2013 AIP Publishing LLC*. [http://dx.doi.org/10.1063/1.4830225]

Magnetoelectric materials, i.e., materials which exhibit a strong interrelation between magnetism and electric polarization, constitute a relatively rare class of compounds with numerous potential applications.[1–4] In these systems a complex interplay between electronic, magnetic, and lattice degrees of freedom takes place. These entangled physical properties pose challenges in understanding the microscopic origin of the manifested magnetoelectricity.[3,4]

One of the most recently discovered series of magnetoelectric materials is the group of ACr$^{3+}_2$X$_4$ spinels (A^{2+} = Zn, Cd, Hg; X^{2-} = O, S, Se; Fig. 1).[5–9] These compounds have been studied extensively over the years, owing to the intimate coupling between their structural, electronic, and magnetic properties.[10–15] These investigations have established the following: (a) The Curie-Weiss temperature Θ_{CW} changes from negative to positive values with increasing lattice constant, or, equivalently, the Cr-Cr distances; the sign of Θ_{CW} changes upon passing from the smaller oxides to the larger chalcogenide spinels. With this variation, the ferromagnetic (FM) exchange interactions are enhanced over the antiferromagnetic (AFM) ones. (b) Even though the FM interactions are predominant in chalcogenides, a strong competition between FM and AFM interactions is present, i.e., bond frustration. Due to this effect, several chalcogenide spinels exhibit complex AFM ground states.[13] (c) Significant spin-phonon coupling is active in these systems near the magnetic ordering temperatures.[13,16–20] Furthermore, coupled magneto-structural transitions are also observed in the AFM ground states.[21,22] (d) Finally, recent studies indicate a close connection between structure and macroscopic electrical polarization for the magnetoelectric members of this family.[20,23] Given this close interrelation between structural, vibrational, magnetic, and charge degrees of freedom, the variation of lattice by external pressure provides an appealing method for tuning the physical properties of these materials. Actually, several studies report structural[24–26] and electronic[26–28] transitions under pressure for various Cr-based spinels.

Here we focus on the high-pressure behavior of the HgCr$_2$S$_4$ spinel, one of the most prominent magnetoelectrics in the Cr-spinel series.[9] In this compound, a strong competition between AFM and FM exchange interactions takes place at ambient pressure.[29] Despite the positive and relatively large value of Θ_{CW}, HgCr$_2$S$_4$ exhibits AFM ordering at 22 K. Furthermore, macroscopic electrical polarization is manifested below 70 K, where strong ferromagnetic fluctuations are present.[9] Since there is no evidence for a structural deviation from the centrosymmetric cubic Fd-$3m$ phase down to 5 K,[16] the origin of the observed polar moments remains puzzling. Nevertheless, HgCr$_2$S$_4$ is suspected to be near a structural instability at ambient pressure already,[29] which makes it an attractive candidate for possible pressure-induced structural effects. Our study reveals that the compression of HgCr$_2$S$_4$ induces several phase transitions.

Details of the HgCr$_2$S$_4$ sample synthesis can be found in Ref. 29. Pressure was generated by a symmetric diamond anvil cell with 300 μm culet diamonds. The ruby luminescence method was employed for measuring pressure.[30] The high-pressure XRD measurements were performed at the 16BM-D beamline of the High Pressure Collaborative Access Team, at the Advanced Photon Source of Argonne National Laboratory. Neon served as pressure transmitting medium (PTM). The measured XRD diffractograms were processed with the FIT2D software.[31] Refinements were performed using the GSAS+EXPGUI software packages.[32,33] For the high-pressure Raman experiments, both helium and a mixture of methanol-ethanol-water 16:3:1 served as PTM in separate runs. The local spin density approximation (LSDA)-based band structure and magnetic exchange calculations were

a)Email: efthymio@oakland.edu
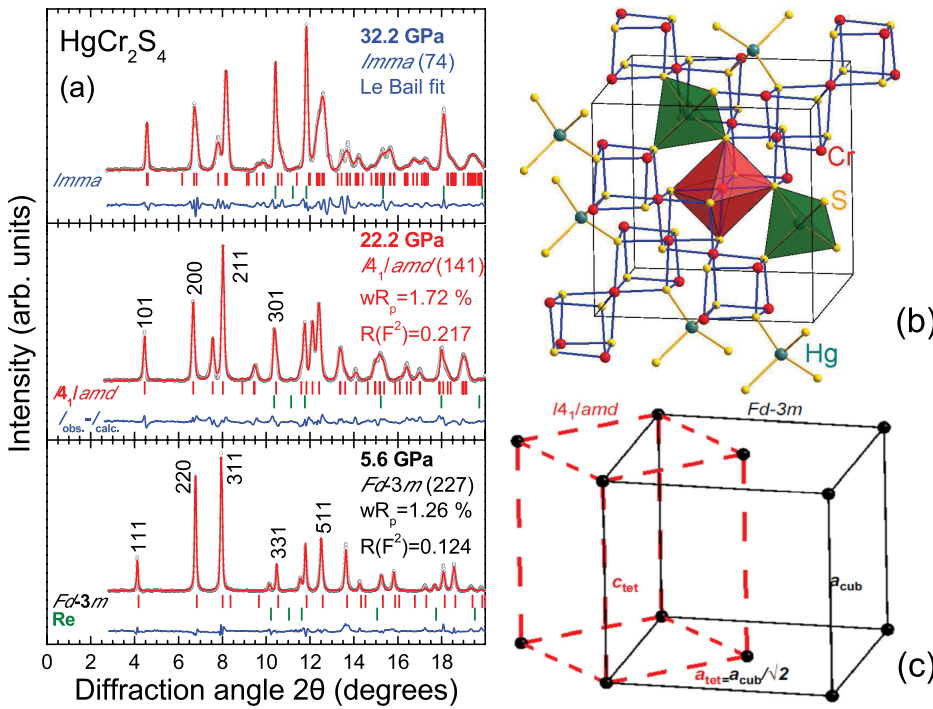b)Author to whom correspondence should be addressed. Electronic mail: ywang235@oakland.edu

FIG. 1. (a) Refined XRD patterns of HgCr$_2$S$_4$ at 5.6 GPa (bottom), at 22.2 GPa (middle), and at 32.2 GPa (top). (b) Unit cell of HgCr$_2$S$_4$ at ambient conditions (SG Fd-$3m$, $Z = 8$). The green, red, and yellow spheres correspond to Hg, Cr, and S ions, respectively. (c) Geometrical relationship between the unit cells of the cubic Fd-$3m$ spinel phase (solid black lines) and the high-pressure tetragonal $I4_1/amd$ structure (dashed red lines).

performed for the experimentally determined crystal structures using the Linear Muffin-tin Orbitals (LMTO) method,[34] which is implemented in the PY LMTO computer code.[35] A thorough description of the theoretical methods utilized in this work can be found in Refs. 14 and 36.

Figure 1(a) shows refined XRD patterns of HgCr$_2$S$_4$ at selected pressures. Overall, three structural transitions can be observed upon compression (Figs. 1, 2, and S1 in supplementary material[37]): the starting Fd-$3m$ structure transforms into a tetragonal $I4_1/amd$ phase at 20 GPa. This structural transition exhibits first-order character, i.e., a 4% volume change at the transition point [Fig. 2(b)]. Such feature is quite unexpected since SG $I4_1/amd$ is a direct subgroup of the starting SG Fd-$3m$. Upon further pressure increase, an orthorhombic distortion of the tetragonal cell occurs at about 27 GPa. This orthorhombic distortion is evidenced mainly by the splitting of the tetragonal (200) Bragg peak.[37] Finally, HgCr$_2$S$_4$ undergoes a third structural transition above 37 GPa (HP3 phase). However, due to the contamination of the XRD patterns with the Bragg peaks of the PTM and the rhenium gasket,[37] the HP3 phase could not be identified. Decompression leads to the back-transformation of the starting Fd-$3m$ structure.[37] In general, the observed sequence of pressure-induced structural transitions in HgCr$_2$S$_4$ is consistent with the trends of several spinels upon compression.[24,38] Here we mainly describe the most interesting high-pressure effect, namely, the Fd-$3m$-$I4_1/amd$ transition.

The tetragonal $I4_1/amd$ structure is not uncommon in the spinel family; various spinels adopt this phase, e.g., at low temperatures upon entering an AFM state[22] or even at ambient conditions due to Jahn-Teller effects.[39] The Fd-$3m$-$I4_1/amd$ transition in these cases, however, does not exhibit any volume change. On the contrary, the cubic-to-tetragonal transformation in our case exhibits a 4% volume reduction [Fig. 2(b)]. In addition, a significant change in the shape of the CrS$_6$ octahedra is taking place: the octahedra

become compressed along c-axis whereas they are expanded within the tetragonal ab-plane. This is evidenced in Fig. 2(d) by the behavior of the two distinct Cr-S bonds in the $I4_1/amd$ phase. In particular, the Cr-S(1) bonds, which refer to the apical S(1) ions along c-axis, adopt a $\sim$3.8% smaller value than the equatorial Cr-S(2) bond distance. This "squeezing" configuration of the CrS$_6$ octahedra is directly linked to electronic effects as it leads to an orbital reconfiguration of the Cr-3d electronic states [inset of Fig. 4(b)].
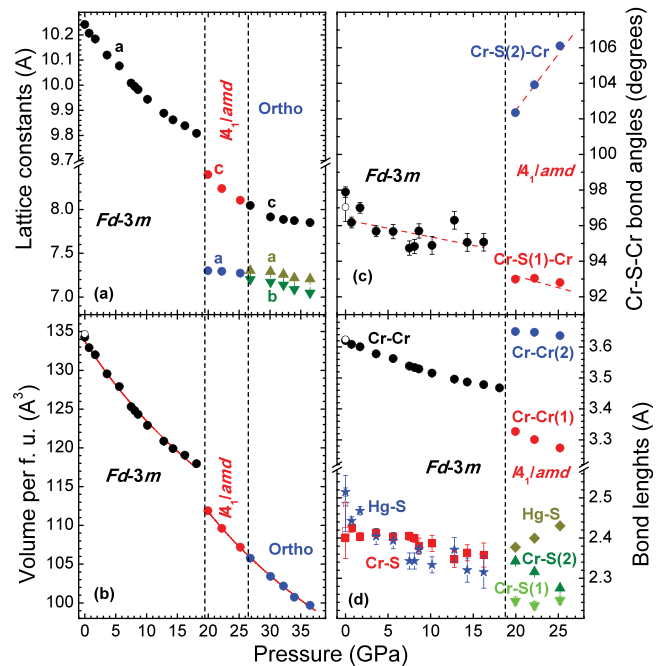
FIG. 2. (a) Lattice constants and (b) unit cell volume per formula unit as a function of pressure for the various phases of HgCr$_2$S$_4$. The vertical dashed lines mark the structural transitions. The pressure-induced changes of (c) the Cr-S-Cr bond angles and (d) selected bond lengths (Cr-Cr, Cr-S, and Hg-S) for the cubic Fd-$3m$ and the tetragonal $I4_1/amd$ phases are also presented.
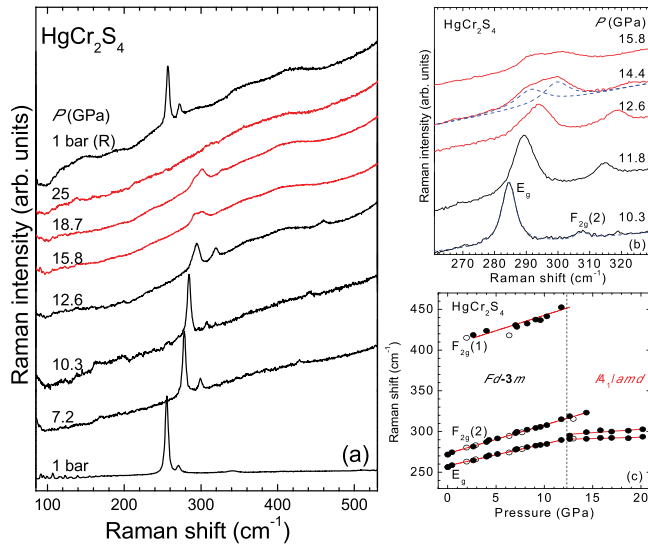
FIG. 3. (a) Raman spectra of $HgCr_2S_4$ at various pressures ($\lambda = 532$ nm, $T = 300$ K). The black and red spectra correspond to the Fd-$3m$ and the $I4_1/amd$ phases, respectively. (b) Raman spectra of $HgCr_2S_4$ in the vicinity of the Fd-$3m$–$I4_1/amd$ structural transition. The blue dashed lines represent Lorentzian fittings. (c) Raman mode frequency evolution as a function of pressure. Closed and open circles represent measurements upon increasing and decreasing pressure, respectively.

Interestingly, similar first-order Fd-$3m$-$I4_1/amd$ structural transitions were observed recently for the $FeCr_2O_4$ (Ref. 24) and $MgCr_2O_4$ (Ref. 25) spinels under pressure. In $FeCr_2O_4$, the first-order character of the transition was attributed to a pressure-induced Jahn-Teller effect of the Fe^{2+} cations residing in the FeO_4 tetrahedra.[24] For the $MgCr_2O_4$ and $HgCr_2S_4$ compounds with orbitally inactive Mg^{2+} and Hg^{2+} cations, however, this explanation seems unlikely.

Our high-pressure Raman spectroscopic measurement revealed that a phase transition is occurring at $\sim$13 GPa (Fig. 3), evidenced by a significant reduction in the overall Raman cross section [Fig. 3(a)] and the splitting of the more intense E_g peak [Figs. 3(b) and 3(c)]. Taking into account our XRD study, we attribute these changes to the Fd-$3m$-$I4_1/amd$ structural transition. We should note here that the lower

transition pressure P_{Tr} evidenced in the Raman study as compared with that of XRD is not unusual in high-pressure experiments; such differences can be accounted for by the different sensitivity of each experimental technique, with Raman spectroscopy probing more local-range order compared to XRD in solids. Since the Raman experiments have been performed with helium as PTM, any non-hydrostatic effects can most likely be excluded as the cause of this 7 GPa P_{tr} difference.

Coming back to the Fd-$3m$-$I4_1/amd$ structural transition, the splitting of the E_g mode is consistent with such transformation.[40] On the other hand, the substantial reduction of Raman intensity *may* indicate pressure-induced modifications of the electronic properties of $HgCr_2S_4$, e.g., an insulator-to-metal transition. Such scenario appears plausible if we take into account the following: (a) $HgCr_2S_4$ exhibits a change from semiconducting to metal-like behavior at ambient pressure upon lowering temperature,[9] (b) the reduced Raman cross section of metallic systems compared to insulators,[41] and (c) the pressure-induced insulator-to-metal transitions reported for $HgCr_2Se_4$ (Refs. 27 and 28) and $FeCr_2S_4$ (Ref. 26) spinel compounds. In order to verify this assumption, we have conducted band structure calculations on $HgCr_2S_4$ for both the Fd-$3m$ and the high-pressure $I4_1/amd$ phases.

In Fig. 4(a) we show the pressure dependence of non-spin-polarized densities of states (DOS) for the Fd-$3m$ structure. Electronic states at the Fermi level (E_F) and at $\sim$2 eV are formed mainly by Cr-$3d$ t_{2g} and e_g states. The former are split by the trigonal component of the ligand field into a_{1g} and $e_{g'}$ states, but the splitting is weak and is neglected in the following discussion. The S-p states form bands below -1 eV but hybridize strongly with the Cr t_{2g} and, especially, the e_g states. As expected, the widths of both Cr-d and S-p states increase with pressure. On the other hand, the narrow sharp peak formed at E_F by the Cr t_{2g} states decreases with pressure; its position, however, is pressure independent. A high DOS at E_F usually points to a structural or magnetic instability. Indeed, if spin polarization is allowed, Hund's coupling immediately splits the half-filled Cr t_{2g} states into completely filled majority- and empty minority-spin states, thus reducing DOS at E_F to zero [Fig. 5(a)].
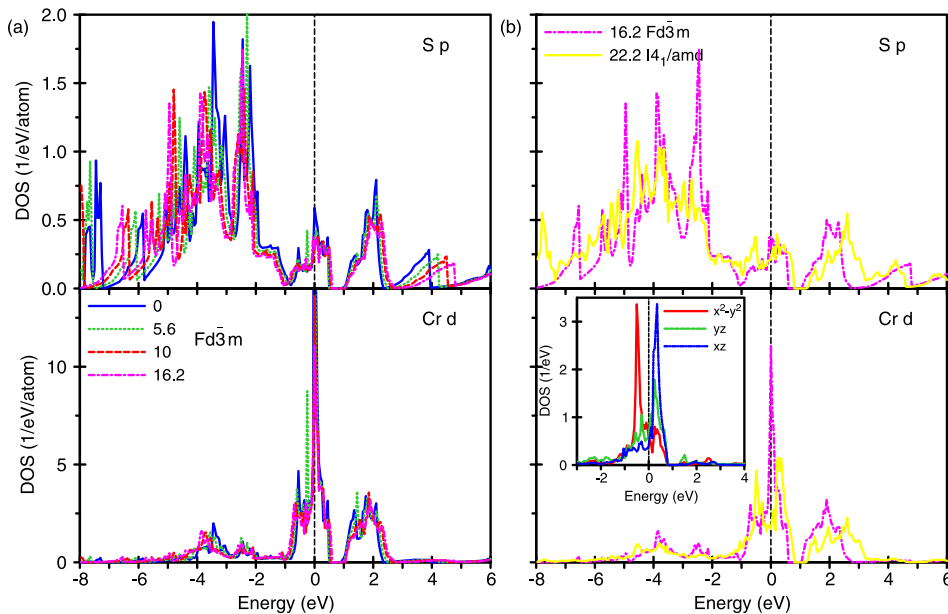

FIG. 4. (a) Calculated DOS for the Fd-$3m$ structure of $HgCr_2S_4$ at selected pressures. The Cr-d and S-p electronic states are presented separately. The Fermi energy (E_F) is assumed at zero. (b) Comparison between the calculated DOS for the Fd-$3m$ (16.2 GPa) and the high-pressure $I4_1/amd$ (22.2 GPa) structures of $HgCr_2S_4$.
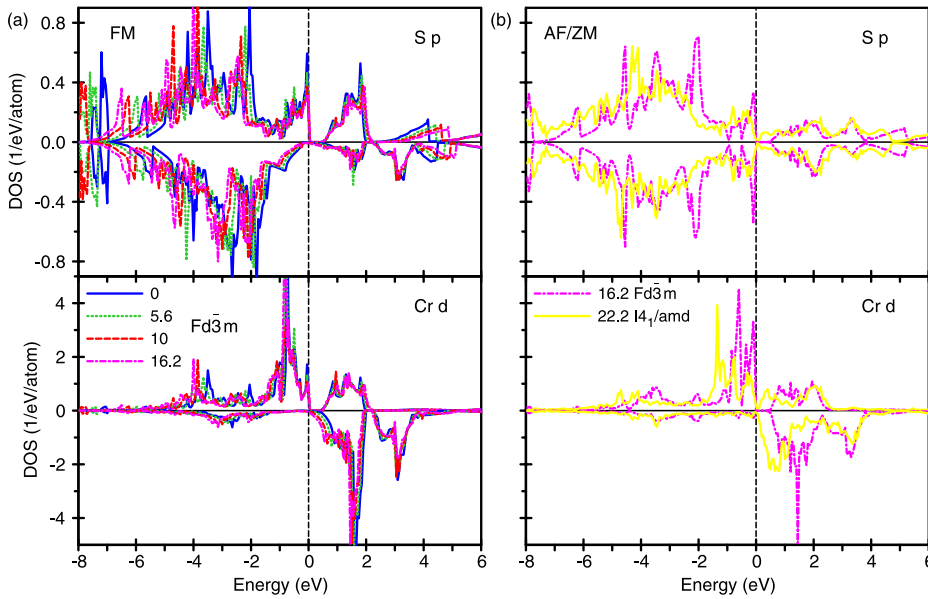
FIG. 5. (a) Spin-polarized DOS for the FM solution (*Fd-3m* structure) of $HgCr_2S_4$ at selected pressures. The Cr-*d* and S-*p* electronic states are presented separately. The Fermi energy (E_F) is assumed at zero. (b) Comparison between the LSDA DOS for the ZM *Fd-3m* solution (16.2 GPa) and the high-pressure AFM $I4_1/amd$ phase (22.2 GPa) of $HgCr_2S_4$.

In Fig. 4(b), the non-spin-polarized DOS curves calculated for the *Fd-3m* structure at $P = 16.2$ GPa are compared to the DOS of the high-pressure $I4_1/amd$ structure ($P = 22.2$ GPa). The most striking differences are the lifting of the degeneracy of the Cr-*d* t_{2g} orbitals as well as the strong decrease of DOS at E_F upon adopting the tetragonal $I4_1/amd$ structure. As shown in the inset of Fig. 4(b), one of Cr-*d* t_{2g} orbitals, $x^2 - y^2$ (*xy* in the cubic notation), becomes almost completely filled. The two other Cr-*d* t_{2g} orbitals (*xz* and *yz*) shift to higher energies due to the stronger compression of the CrS_6 octahedron along *z*-axis in the $I4_1/amd$ structure [Fig. 2(d)]. This DOS decrease indicates a tendency to suppress magnetism in the $I4_1/amd$ phase.

In order to unveil the effect of pressure on the magnetic properties of the *Fd-3m* phase of $HgCr_2S_4$, we performed spin-polarized LSDA calculations for spin-spiral structures with a wave vector **q** varying along [00*q*] and [*qq*0] lines. Obviously, the spiral with $q = 0$ gives FM order of Cr moments. Collinear antiferromagnetic order, which results in the total spin per Cr_4 tetrahedron equal to zero (ZM), is realized by spirals with $q = 2$ in $2\pi/a$ unit, where *a* is the cubic lattice constant. Such order gives the lowest magnetic energy if the dominant exchange interaction is AFM nearest-neighbor coupling j_1. Calculations were also performed for a *non-collinear* spin structure with Cr moments directed along the lines passing through the center of a Cr_4 tetrahedron, which also gives zero total spin per tetrahedron.[37] The total energies calculated for the two spin structures with zero total moment are equal within numerical accuracy.

At ambient pressure the FM structure is more stable than the ZM one, indicating that the dominant exchange interaction is FM.[37] However, due to competition with a rather strong AFM exchange interaction j_3 between 3-rd Cr neighbors, the total energy minimum is found at an incommensurate wave vector $\mathbf{q}_{min} = (0,0,0.6)$. Under pressure the energy difference between the ZM and FM spin structures gradually decreases, and the ZM solution becomes lower in energy at 16.2 GPa. The total energy minimum shifts to larger $\mathbf{q}_{min} = (0,0,1.05)$. Thus, the dominant exchange interaction becomes less ferromagnetic, or even changes sign from FM to AFM with

increasing pressure in the *Fd-3m* phase of $HgCr_2S_4$. This behavior can be explained by the strong increase of AFM contribution to j_1 due to the decrease of Cr-Cr distances under pressure[14,36] and is consistent with the experimental high-pressure magnetic studies of Cr-spinels.[42,43]

The spin-polarized Cr-*d* and S-*p* DOS of the FM *Fd-3m* phase are shown in Fig. 5(a), and the DOS curves for the ZM solution ($P = 16.2$ GPa) are displayed in Fig. 5(b). The LSDA calculations for the FM ordering of Cr moments (*Fd-3m*) yield a metallic solution for all pressures. The only apparent change in the $HgCr_2S_4$ FM DOS upon increasing pressure is the increasing overlap between the bottom of minority-spin and the top of the majority-spin Cr-*d* t_{2g} bands. It is worth mentioning that the $HgCr_2S_4$ FM solution remains metallic even in the LSDA+U calculations; a tiny gap opens at E_F for minority-spin bands only for $U = 4$ eV.

For the ZM *Fd-3m* structure of $HgCr_2S_4$, a gap of $E_g = 0.34$ eV is obtained [Fig. 5(b)]. The ZM gap is smaller than the experimental value $E_g \sim 1$ eV of $HgCr_2S_4$ at ambient pressure.[12] In LSDA+U calculations for the ZM solution with $U = 3$ and 4 eV, the E_g value increases to 0.74 eV and 0.86 eV, respectively.

More spectacular behavior is found for spin spirals: at ambient pressure the solution with the wave vector equal to $\mathbf{q}_{min}$ is insulating, with an indirect gap equal to 0.14 eV and a somewhat larger direct gap of 0.20 eV. At $P = 5.6$ GPa the gaps decrease to 0.10 and 0.19 eV, respectively, whereas beyond $P = 10$ GPa the solution with the wave vector $\mathbf{q}_{min}$ becomes metallic. This finding correlates well with the observed reduction of Raman intensity after the *Fd-3m*-$I4_1/amd$ structural transition [Fig. 3]. Therefore, our assumption for an insulator-to-metal transition accompanying the *Fd-3m*-$I4_1/amd$ structural modification in $HgCr_2S_4$ appears reasonable.

Spin-polarized calculations were also performed for the high-pressure $I4_1/amd$ phase of $HgCr_2S_4$ [Fig. 5(b)]. In this case spin spirals with wave vectors (*q*00) and (00*q*) are no longer equivalent, with the latter being more favorable due to shortening of Cr-Cr distances along AFM bonds.[37] The lowest total energy was calculated for a spiral with

$q_{min} \sim (0,0,1.0)$. It should be pointed out that the energy gain due to formation of a magnetic solution gradually decreases with increasing pressure.[37] It appears that pressure increase favors a non-magnetic solution, thus leading subsequently to a complete suppression of magnetism for $HgCr_2S_4$.

Finally, we discuss the possible effects of pressure on the electrical polarization of $HgCr_2S_4$. Recent microstructural studies on magnetoelectric $CdCr_2S_4$ suggest that ferroelectricity arises due to the "dynamic" off-centering of the Cr^{3+} cations.[20,23] This cationic off-centering alters the local structure from Fd-$3m$ to $F4$-$3m$, which "permits" the appearance of macroscopic electrical polarization. Such idea was put forward many years ago for Cr-spinels.[44] Therefore, it is only reasonable to assume that ferroelectricity in both $HgCr_2S_4$ and $CdCr_2S_4$ compounds share the same origin, i.e., local displacements of the magnetic Cr^{3+} cations. In an intuitive manner, one expects that application of pressure will suppress these ionic displacements and concomitantly will suppress ferroelectricity, a well-documented effect for "traditional" ferroelectrics.[45,46] We should note here that the high-pressure $I4_1/amd$ phase of $HgCr_2S_4$ is again centrosymmetric, thus (in principle) excluding any ferroelectricity. Given also that compression favors a non-magnetic ground state for $HgCr_2S_4$, it appears that application of pressure is detrimental for magnetoelectricity in this system.

In conclusion, we have observed a rich phase diagram for the magnetoelectric $HgCr_2S_4$ spinel under compression at ambient temperature. The first structural transition (Fd-$3m$-$I4_1/amd$) appears to be accompanied by modifications in both the electronic and magnetic properties of the material, as revealed by our Raman and theoretical studies. Finally, the adoption of the $I4_1/amd$ phase under pressure seems detrimental for the magnetic and, hence, magnetoelectric properties of $HgCr_2S_4$.

[1]S.-W. Cheong and M. Mostovoy, Nat. Mater. **6**, 13 (2007).
[2]D. I. Khomskii, J. Magn. Magn. Mater. **306**, 1 (2006).
[3]S. Picozzi and A. Stroppa, Eur. Phys. J. B **85**, 240 (2012).
[4]K. F. Wang, J.-M. Liu, and Z. F. Ren, Adv. Phys. **58**, 321 (2009).
[5]J. Hemberger, P. Lunkenheimer, R. Fichtl, H.-A. von Nidda, V. Tsurkan, and A. Loidl, Nature **434**, 364 (2005).
[6]J. Hemberger, P. Lunkenheimer, R. Fichtl, S. Weber, V. Tsurkan, and A. Loidl, Physica B **378**, 363 (2006).
[7]H. Murakawa, Y. Onose, K. Ohgushi, S. Ishiwata, and Y. Tokura, J. Phys. Soc. Jpn. **77**, 43709 (2008).
[8]K. Siratori and E. Kita, J. Phys. Soc. Jpn. **48**, 1443 (1980).
[9]S. Weber, P. Lunkenheimer, R. Fichtl, J. Hemberger, V. Tsurkan, and A. Loidl, Phys. Rev. Lett. **96**, 157202 (2006).
[10]P. K. Baltzer, P. J. Wojtowicz, M. Robbins, and E. Lopatin, Phys. Rev. **151**, 367 (1966).
[11]P. Bruesch and F. D'Ambrogio, Phys. Status Solidi **50**, 513 (1972).
[12]H. W. Lehmann and G. Harbeke, Phys. Rev. B **1**, 319 (1970).
[13]T. Rudolf, C. Kant, F. Mayr, J. Hemberger, V. Tsurkan, and A. Loidl, New J. Phys. **9**, 76 (2007).
[14]A. N. Yaresko, Phys. Rev. B **77**, 115106 (2008).
[15]O. Hartmann, G. M. Kalvius, R. Wappling, A. Gunther, V. Tsurkan, A. Krimmel, and A. Loidl, Eur. Phys. J. B **86**, 148 (2013).
[16]T. Rudolf, C. Kant, F. Mayr, J. Hemberger, V. Tsurkan, and A. Loidl, Phys. Rev. B **76**, 174307 (2007).
[17]T. Rudolf, C. Kant, F. Mayr, J. Hemberger, V. Tsurkan, and A. Loidl, Phys. Rev. B **75**, 52410 (2007).
[18]A. B. Sushkov, O. Tchernyshyov, W. Ratcliff II, S. W. Cheong, and H. D. Drew, Phys. Rev. Lett. **94**, 137202 (2005).
[19]J. Hemberger, T. Rudolf, H.-A. K. von Nidda, F. Mayr, A. Pimenov, V. Tsurkan, and A. Loidl, Phys. Rev. Lett. **97**, 87204 (2006).
[20]V. Gnezdilov, P. Lemmens, Y. G. Pashkevich, C. Payen, K. Y. Choi, J. Hemberger, A. Loidl, and V. Tsurkan, Phys. Rev. B **84**, 45106 (2011).
[21]S.-H. Lee, G. Gasparovic, C. Broholm, M. Matsuda, J.-H. Chung, Y. J. Kim, H. Ueda, G. Xu, P. Zschack, K. Kakurai, H. Takagi, W. Ratcliff, T. H. Kim, and S.-W. Cheong, J. Phys.: Condens. Matter **19**, 145259 (2007).
[22]F. Yokaichiya, A. Krimmel, V. Tsurkan, I. Margiolaki, P. Thompson, H. N. Bordallo, A. Buchsteiner, N. Stuesser, D. N. Argyriou, and A. Loidl, Phys. Rev. B **79**, 64423 (2009).
[23]G. N. P. Oliveira, A. M. Pereira, A. M. L. Lopes, J. S. Amaral, A. M. dos Santos, Y. Ren, T. M. Mendonca, C. T. Sousa, V. S. Amaral, J. G. Correia, and J. P. Araujo, Phys. Rev. B **86**, 224418 (2012).
[24]A. Kyono, S. A. Gramsch, T. Yamanaka, D. Ikuta, M. Ahart, B. O. Mysen, H. K. Mao, and R. J. Hemley, Phys. Chem. Miner. **39**, 131 (2012).
[25]W. Yong, S. Botis, S. R. Shieh, W. Shi, and A. C. Withers, Phys. Earth Planet. Inter. **196–197**, 75 (2012).
[26]Y. Amiel, G. K. Rozenberg, N. Nissim, A. Milner, M. P. Pasternak, M. Hanfland, and R. D. Taylor, Phys. Rev. B **84**, 224114 (2011).
[27]S.-D. Guo and B.-G. Liu, J. Phys.: Condens. Matter **24**, 45502 (2012).
[28]P. Kistaiah, K. S. Murthy, and K. V. K. Rao, J. Less-Common Met. **98**, L13 (1984).
[29]V. Tsurkan, J. Hemberger, A. Krimmel, H.-A. K. von Nidda, P. Lunkenheimer, S. Weber, V. Zestrea, and A. Loidl, Phys. Rev. B **73**, 224442 (2006).
[30]H. K. Mao, J. Xu, and P. M. Bell, J. Geophys. Res. **91**, 4673, doi:10.1029/JB091iB05p04673 (1986).
[31]A. Hammersley, S. Svensson, M. Hanfland, A. Fitch, and D. Hausermann, High Press. Res. **14**, 235 (1996).
[32]B. H. Toby, J. Appl. Crystallogr. **34**, 210 (2001).
[33]R. B. von Dreele and A. C. Larson, Los Alamos National Laboratory Report No. LAUR 86-748, 1994.
[34]O. K. Andersen, Phys. Rev. B **12**, 3060 (1975).
[35]A. Y. Perlov, A. N. Yaresko, and V. N. Antonov (unpublished).
[36]A. V. Ushakov, D. A. Kukusta, A. N. Yaresko, and D. I. Khomskii, Phys. Rev. B **87**, 14418 (2013).
[37]See supplementary material at http://dx.doi.org/10.1063/1.4830225 for a compilation of the measured XRD spectra and the extracted structural data at various pressures, as well as the sketches and plots of the stabilization energies for the various magnetic configurations of $HgCr_2S_4$ considered for the LSDA calculations.
[38]D. Errandonea, R. S. Kumar, F. J. Manjon, V. V. Ursaki, and I. M. Tiginyanu, J. Appl. Phys. **104**, 63524 (2008).
[39]P. G. Radaelli, New J. Phys. **7**, 53 (2005).
[40]C. M. Julien and M. Massot, J. Phys.: Condens. Matter **15**, 3151 (2003).
[41]A. F. Goncharov and V. V. Struzhkin, J. Raman Spectrosc. **34**, 532 (2003).
[42]H. Ueda and Y. Ueda, Phys. Rev. B **77**, 224411 (2008).
[43]Y. Jo, J.-G. Park, H. C. Kim, W. Ratcliff II, and S.-W. Cheong, Phys. Rev. B **72**, 184421 (2005).
[44]N. W. Grimes and E. D. Isaac, Philos. Mag. **35**, 503 (1977).
[45]T. Ishidate, S. Abe, H. Takahashi, and N. Mori, Phys. Rev. Lett. **78**, 2397 (1997).
[46]G. A. Samara, T. Sakudo, and K. Yoshimitsu, Phys. Rev. Lett. **35**, 1767 (1975).